ELSEVIER

Journal of Photochemistry and Photobiology A: Chemistry 151 (2002) 181–193

Journal of Photochemistry and Photobiology A:Chemistry

www.elsevier.com/locate/jphotochem

Fe(III) photoinduced and Q-TiO_2 photocatalysed degradation of naphthalene: comparison of kinetics and proposal of mechanism

Lenka Hykrdová [a,*], Jaromír Jirkovský [a], Gilles Mailhot [b], Michèle Bolte [b]

[a] *J. Heyrovský Institute of Physical Chemistry, Academy of Sciences of the Czech Republic, Dolejškova 3, Prague 182 23, Czech Republic*
[b] *Laboratoire de Photochimie Moléculaire et Macromoléculaire, UMR 6505, Université Blaise Pascal, 63177 Aubière Cedex, France*

Received 30 December 2001; accepted 15 January 2002

Abstract

Degradation of naphthalene was investigated in two systems producing hydroxyl radical: in homogeneous solution of Fe(III) perchlorate and in heterogeneous colloidal solution of Q-TiO_2. The Fe(III) photoinduced degradation of naphthalene approximately followed first order kinetics with rate constant strongly dependent on the content of most photoactive Fe(III) species, $Fe(OH)^{2+}$. In the case of the degradation photocatalysed by Q-TiO_2, more complicated kinetics controlled by a charge-transfer surface complex with naphthalene degradation intermediates was observed. The primary degradation intermediates (2-formylcinnamaldehyde, 1,2-naphthoquinone, 1,4-naphthoquinone, 1-naphthol, 2-naphthol) were the same for both systems. The reaction mechanism of the degradation was proposed assuming the attack of hydroxyl radical followed by the addition of dioxygen, resulting in the direct opening of the aromatic ring.

Keywords: Photoinduced; Photocatalysed; Aromatic ring; Naphthalene

1. Introduction

Recently, largely developed advanced oxidation processes are based on the production of hydroxyl radicals. These highly reactive species attack organic molecules and oxidize them in the presence of oxygen in series of subsequent steps up to CO_2, H_2O and mineral acids. Hydroxyl radicals can be formed in a large number of chemical and photochemical processes. The aim of this work was to study oxidative degradation in two systems that produce hydroxyl radicals under UV–VIS irradiation: in (i) homogeneous aqueous solutions containing Fe(III) salts and (ii) heterogeneous aqueous colloidal dispersions of quantum sized titanium dioxide particles (Q-TiO_2). Both systems are capable to produce hydroxyl radical also under sunlight.

A solution of Fe(III) can contain several mononucleic complexes: $[Fe(H_2O)_6]^{3+}$, $[Fe(H_2O)_5(OH)]^{2+}$, and $[Fe(H_2O)_4(OH)_2]^{+}$, the proportion among them being pH dependent [1]. Monohydroxy complex, $Fe(OH)^{2+}$ (water molecules are omitted for simplicity), is the predominant monomeric species in the solution of Fe(III) perchlorate at pH between 2.5 and 5, i.e. the conditions of our study. In the course of time, monomeric species undergo aging, a process dependent on the concentration of Fe(III), pH, temperature, etc. The changes can be observed by UV–VIS absorption spectroscopy: freshly prepared slightly yellow solution of Fe(III) monomeric species turns progressively to brownish color typical for soluble aggregates [2] (dimers, oligomers, etc.). Under irradiation, $Fe(OH)^{2+}$ photolyzes most efficiently to produce Fe(II) and hydroxyl radical:

$$Fe(OH)^{2+} \xrightarrow{h\nu} Fe^{2+} + OH^{\bullet}$$

For the continuous reoxidation of Fe^{2+}, the presence of molecular oxygen and irradiation are the necessary conditions [3]. The heterogeneous system of colloidal solution of Q-TiO_2 produces hydroxyl radicals following light absorption by semiconductor [4]. Formed electron–hole pairs are separated; holes can be trapped by surface bound hydroxyl group forming hydroxyl radicals. Electrons can be consumed in reactions with electron acceptors, e.g. molecular oxygen, producing superoxide radical anions. The efficiency of these charge-transfer processes is significantly reduced by recombination of the charge carriers inside semiconductor particles.

As a model compound for the photooxidative degradation studies initiated by the attack of hydroxyl radical, naphthalene was chosen. It is the simplest of polyaromatic hydroxycarbons and it occurs in the environment as a pollutant. Its oxidative decomposition has been followed in

* Corresponding author.

1010-6030/02/$ – see front matter
PII: S1010-6030(02)00014-X

various systems producing hydroxyl radical, e.g. in aqueous suspensions of TiO_2 [5–8], with the Fenton's reagent [9], in combination of H_2O_2 and UV irradiation [9,10], in a system of Cu^+/Cu^{2+} redox couple with Pd supported silica as a catalyst, and by photolysis of isopropylnitrite in the presence of NO in the gaseous phase [11–14]. Photolysis of naphthalene in an aqueous solution irradiated at 254 nm was also followed [15].

2. Experimental

All chemicals were used without further purification. Naphthalene was bought from Eastman Kodak Company, NY, scintillation grade. Fe(III) solutions were prepared by dissolution of ferric perchlorate $Fe(ClO_4)_3{\cdot}9H_2O$ (Fluka; >97%) to 2.0×10^{-3} mol l^{-1} by Millipore αQ water. This stock solution was diluted to a desired concentration and used either immediately or after time needed to achieve certain degree of Fe(III) hydrolysis. The quantum sized TiO_2 was prepared by controlled hydrolysis of titanium chloride (Sigma, p.a.) according to the method described by Kormann et al. [16]. The concentration of Q-TiO_2 was adjusted to 33.3×10^{-3} mol l^{-1}. The pH was increased using dialysis to the final value of 2.5 [17]. Kormann et al. [16] found that the mean diameter of such prepared Q-TiO_2 particles was below 3 nm (approximately 200 molecules of TiO_2 per particle) with a crystal structure of anatase. Before performing irradiation experiments, the diluted colloidal solutions of Q-TiO_2 were slightly acidified by the addition of perchloric acid (Merck, p.a.) to the concentration of 10^{-2} mol l^{-1} to prevent precipitation. The particles were used either freshly prepared or aged for 2–4 years.

Determination of the $Fe(OH)^{2+}$ content was made according to the method described by Faust and Hoigné [1] using sodium salt of 8-hydroxyquinoline-5-sulfonic acid (Aldrich, >98%). Fe(II) was determined using complexometry with 0.1% solution of 1,10-phenanthroline (Fluka, puriss >99%) in acetic buffer.

UV–VIS absorption spectra were measured by spectrometers Cary 13 (Varian) or Lambda 19 (Perkin-Elmer). The HPLC analyses were performed by the means of instruments Waters 510 system (with autosampler Waters 717 and diode array detector Waters 996) and Merck L-6200 A (with UV–VIS absorption detector L-4250 and integrator D-2500). A chromatographic column with reverse phase, Lichrospher RP 18 (250 mm × 4.6 mm (i.d.), 5 μm (p.d.), 100 Å), was employed. Naphthalene was determined by HPLC using isocratic elution with 90% acetonitrile and 10% water; flow rate 1 ml min^{-1}, injection 20 μl; detection wavelength 276 nm. For the separation of degradation products, gradient elution with the following solvents was applied: (**A**) H_2O (Millipore) with 0.1% H_3PO_4, and (**B**) acetonitrile (Carlo Erba reagenti, 99.9%). The flow rate was 1 ml min^{-1}, injection 50 or 100 μl, detection at 240 nm and a gradient program: 0 min: 90% **A**, 5 min: 90% **A**, 30 min: 0% **A**.

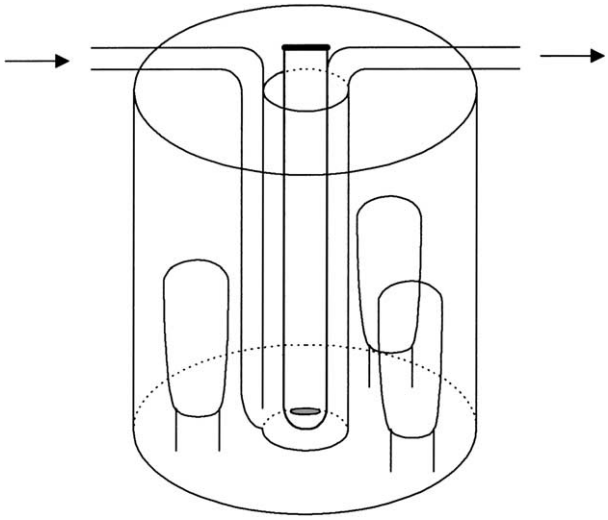

Fig. 1. Scheme of the irradiation setup (with three "black" lamps built on a circular base). The arrows indicate the flow of cooling water.

Degradation experiments were performed in containers made of stainless steel cylinders, built upon a circular or elliptical base. The solution (up to 100 ml) was irradiated in a Pyrex glass tube. In the first case, it was placed vertically in the center of the cylinder and irradiated by medium pressure mercury lamps (RVU, Tesla Holešovice, 125 W) as shown in Fig. 1. For the second arrangement, one medium pressure mercury lamp (Mazda MAW type 125 W) was centered at a focal axis of the elliptical container and the photoreactor tube was located at the other focal axis. In both cases, the lamps emitted dominantly at 365 nm. The photoreactor tubes were placed in a Pyrex glass jacket of a slightly larger diameter flushed by water; thus providing cooling and keeping constant temperature of the irradiated solution. The incident light intensity measured with potassium ferrioxalate according to the method described by Calvert and Pitts [18] was $I_0 = 1.0 \times 10^{16}$ photons s^{-1} cm^{-3} (70 ml of irradiated solution) for the former photoreactor (one lamp operating), and 4.5×10^{15} photons s^{-1} cm^{-3} (60 ml of irradiated solution) for the latter photoreactor.

Quantum yields were measured using a Bausch and Lomb monochromator and a high pressure mercury lamp (Osram HBO 200 W) for irradiation. A sample (3 ml) was placed in a square quartz spectroscopic cell (optical path 1 cm) and magnetically stirred. The incident light intensities were measured also by ferrioxalate actinometry [18].

3. Results and discussion

3.1. Fe(III) photoinduced degradation of naphthalene

3.1.1. Course of the degradation

The composition of Fe(III) solutions changed in time due to hydrolysis and oligomerization processes. While

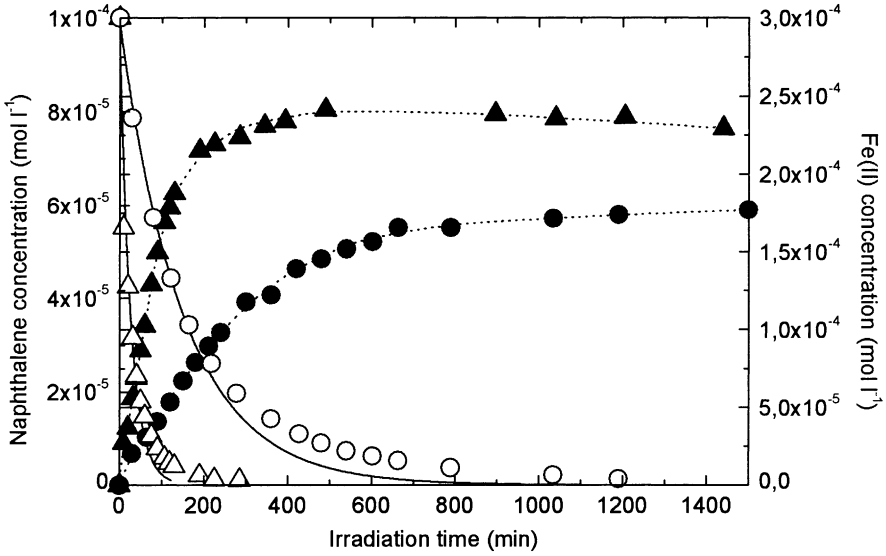

Fig. 2. Degradation of 1.0×10^{-4} mol l^{-1} naphthalene photoinduced by 3.0×10^{-4} mol l^{-1} $Fe(ClO_4)_3$ at various initial contents of Fe(III) monomeric species: (○), naphthalene, 21% of monomeric species; (△), naphthalene, 97% of monomeric species; (●), iron(II), 21% of monomeric species; (▲), iron(II), 97% of monomeric species. The full lines represent first order fits for several first experimental points.

the content of $Fe(OH)^{2+}$ in freshly prepared solution of 3×10^{-4} mol l^{-1} $Fe(ClO_4)_3$ decreased from 95 to 30% after 1 h, following approximately first order kinetics, the optical density of the same solution measured at 365 nm in 1 cm cell changed from 0.096 to 0.525. These changes corresponded to the formation of oligomeric forms of Fe(III) that have their spectral maxima at longer wavelengths [2]. The hydrolytic and oligomerization processes controlled the proportion among Fe(III) species that differed in their photoactivities and thus impacted the rate of hydroxyl radical production. In addition, the overall concentration of Fe(III) decreased during irradiation due to its reduction to Fe(II).

In Fig. 2, the experimental data of naphthalene degradation for two different initial contents of monomeric Fe(III) are compared with first order fits of several first experimental points. The rate constants resulted from these fits were used to calculate initial reaction rates of naphthalene degradation: $(1.1 \pm 0.1) \times 10^{-4}$ s^{-1} for the initial content of 21% of Fe(III) monomeric species, and $(6.1 \pm 0.6) \times 10^{-4}$ s^{-1} for the initial content of 97% of Fe(III) monomeric species. Besides the naphthalene determination, Fe(II) content in the irradiated reaction mixture was continuously analyzed. A good agreement with the diminution of naphthalene was found. At initial stages, the rates of Fe(II) formation were high and then they slowed down; finally, the concentration of Fe(II) reached constant photostationary values different for both initial contents of monomeric Fe(III).

During the irradiation process, Fe(II) ions had to be obviously continuously reoxidized to Fe(III). This might proceed via reactions of Fe(II) with oxidizing species that could occur in the aerated irradiated reaction mixture, such as hydroxyl radicals, OH-adducts, hydroperoxyl radicals, H_2O_2, peroxyl radical [19,20], organic peroxides [21], endoperoxides, tetraoxides, etc. Also a direct photooxidation of Fe(II) by molecular oxygen that was described by Sarakha et al. [3] should participate.

3.1.2. Determination of quantum yields

Quantum yields of both naphthalene degradation and Fe^{2+} formation were studied as functions of irradiation wavelength and initial content of monomeric Fe(III). Due to slow solubilization of naphthalene in water and its high volatility, these solutions were prepared by addition of concentrated stock solution of naphthalene in acetonitrile into aqueous solution of $Fe(ClO_4)_3$ so that they contained 1.0×10^{-4} mol l^{-1} naphthalene and 3×10^{-4} mol l^{-1} $Fe(ClO_4)_3$. The final acetonitrile concentration was 1% (0.24 mol l^{-1}). The rate constant of the reaction of hydroxyl radical with acetonitrile, $k_{CH_3CN} = 2.2 \times 10^7$ l mol^{-1} s^{-1} is much lower than that with naphthalene [22], $k_N = 1.2 \times 10^{10}$ l mol^{-1} s^{-1}. Even though the products $k_{CH_3CN}[CH_3CN]$ and $k_N[N]$ are of the same order of magnitude, no changes in composition of photoproducts were observed in the presence of acetonitrile.

The starting $Fe(OH)^{2+}$ percentage influenced the initial rates of both naphthalene degradation and Fe^{2+} formation. The quantum yields of naphthalene degradation, Φ_N, as well as Fe^{2+} formation, $\Phi_{Fe^{2+}}$, were measured for constant $Fe(ClO_4)_3$ concentration but different initial percentages of $Fe(OH)^{2+}$. The results are reported in Table 1. Both quantum yields markedly decreased with decreasing $Fe(OH)^{2+}$ content which indicates that the percentage of $Fe(OH)^{2+}$ species was the most important factor influencing the quantum yields. These findings correspond with the previously reported results [21,23].

The values of $\Phi_{Fe^{2+}}$ are higher than those of Φ_N. Similar results were found in studies dealing with

Table 1
Dependence of quantum yields of naphthalene degradation, Φ_N, and Fe^{2+} formation, $\Phi_{Fe^{2+}}$, on initial $Fe(OH)^{2+}$ content for irradiation wavelength of 365 nm. The solutions contained 3×10^{-4} mol l^{-1} $Fe(ClO_4)_3$, 1.0×10^{-4} mol l^{-1} naphthalene and 1% acetonitrile

$Fe(OH)^{2+}$ (%)	Φ_N	$Fe(OH)^{2+}$ (%)	$\Phi_{Fe^{2+}}$
6	0.0012	12	0.0081
15	0.0010	19	0.0077
50	0.0044	50	0.014
97	0.024	90	0.090

Fe(III) photoinduced degradation of other compounds [23].

The dependence of the quantum yields on the irradiation wavelength was measured for the starting content of 50% $Fe(OH)^{2+}$. The results are listed in Table 2. The Φ_N and $\Phi_{Fe^{2+}}$ increased with the decreasing excitation wavelength up to 300 nm. That corresponds to the variation of probability of Fe–OH dissociation when $Fe(OH)^{2+}$ is excited to higher vibration states of the first excited electronic state. The further increase of Φ_N at shorter wavelengths can be attributed to the direct photolysis of naphthalene. The quantum yield of naphthalene photolysis was estimated to be $\Phi_{N,photolysis} = 0.037$ at 254 nm. The latter value, $\Phi_{Fe^{2+}}$, became more or less constant at shorter wavelengths. As the absorbances of naphthalene and Fe(III) at these wavelengths became similar in the used solution, the competitive absorption of naphthalene had to reduce reaction rates of the photoinduced processes.

3.1.3. Intermediates of Fe(III) photoinduced degradation of naphthalene

The formation of degradation intermediates of naphthalene in aqueous solution was followed by the means of HPLC with UV–VIS absorption detection. Over 50 intermediates were detected in the irradiated solutions, with retention times shorter than that of naphthalene. This would suggest the formation of more polar, oxygen-containing products. Employing HPLC coupled with MS technique, a high response of also other compounds of lower molecular mass was observed. These components of the reaction mixture probably corresponded to further degraded intermediates with opened aromatic rings that do not absorb light over 220 nm and thus gave no response with the UV–VIS absorption detection.

Applying flash photolysis technique (Nortech FPX-1 flash lamp emitting energy of 130 J, with a rise time of 10 μs, equipped with a cut-off filter, $\lambda > 320$ nm) to the solution containing 1.0×10^{-4} mol l^{-1} naphthalene and 3.0×10^{-4} mol l^{-1} Fe(III), two main primary intermediates with a very high abundance, 2-formylcinnamaldehyde (**I**) and 1,2-naphthoquinone (**II**), appeared after the first flash. In smaller amounts, 1,4-naphthoquinone **(III)**, 1-naphthol (**IV**), and 2-naphthol (**V**) were also present.

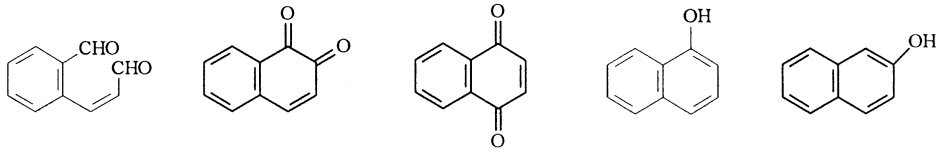

(I) **(II)** **(III)** **(IV)** **(V)**

The concentration of intermediates was followed in the course of degradation of 1.0×10^{-4} mol l^{-1} naphthalene photoinduced by 3.0×10^{-4} mol l^{-1} Fe(III) perchlorate. The time profiles of the primary intermediates are plotted in Fig. 3. Among further degradation intermediates, phthalic acid, *o*-formylbenzoic acid, 7-hydroxy-1,4-naphthoquinone could be unambiguously identified employing comparison with corresponding standard products.

Another set of experiments was performed to clarify the role of naphthols in the degradation pathway of naphthalene. Naphthols were proposed to be the only primary intermediates following an attack of hydroxyl radical to naphthalene during its photocatalytic degradation in TiO_2 slurries [6]. We observed that thermal reactions occurred between naphthols and Fe(III). The reaction between 1-naphthol and Fe(III) yielded a mixture of oligomeric intermediates as found by HPLC/UV–VIS. Using UV–VIS absorption spectroscopy, formation of a complex between these intermediates and Fe(III) was observed. In case of the thermal reaction of 2-naphthol with Fe(III), only one predominant product was formed. It was identified as 1,1′-binaphthyl-2,2′-diol using HPLC coinjection with a commercial standard. However, thermal reactions of 2-naphthol proceeded much slower. After 120 min, only 25% of 2-naphthol reacted while almost complete (99%) conversion of 1-naphthol was achieved in the same time.

The fast thermal reaction disabled to perform experiments with the photoinduced degradation of 1-naphthol. In case of 2-naphthol, 1,2-naphthoquinone and phthalic acid were found in the reaction mixture in minor amounts

Table 2
Dependence of quantum yields of naphthalene degradation, Φ_N, and Fe^{2+} formation, $\Phi_{Fe^{2+}}$, on irradiation wavelength for initial content of 50% $Fe(OH)^{2+}$. The solutions contained 3×10^{-4} mol l^{-1} $Fe(ClO_4)_3$, 1.0×10^{-4} mol l^{-1} naphthalene and 1% acetonitrile

Wavelength (nm)	Φ_N	$\Phi_{Fe^{2+}}$
365	0.0044	0.023
334	0.020	0.056
313	0.022	0.088
296	0.028	0.088
254	0.057	0.093

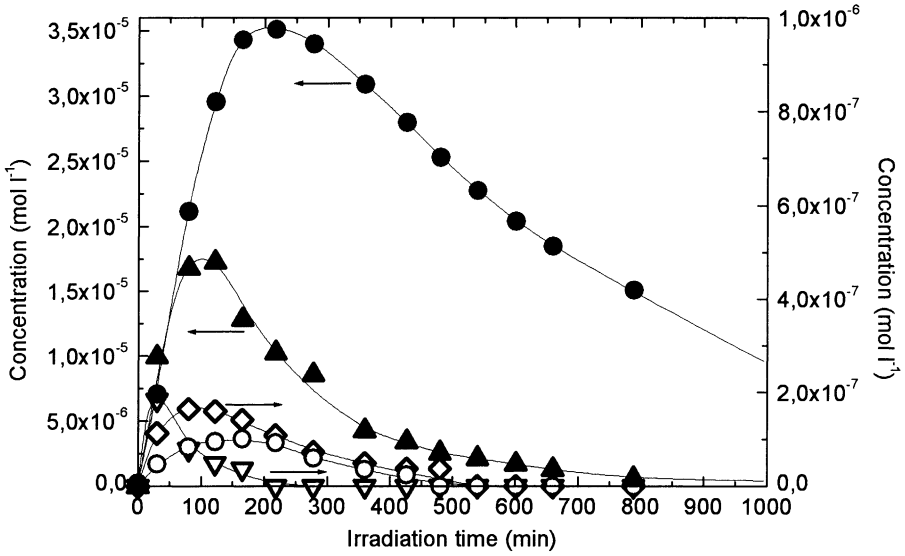

Fig. 3. Time profiles of primary intermediates of degradation of 1.0×10^{-4} mol l^{-1} naphthalene photoinduced by 3.0×10^{-4} mol l^{-1} $Fe(C1O_4)_3$ for initial content of 21% of Fe(III) monomeric species. Left axis: (●), 2-formylcinnamaldehyde; (▲), 1,2-naphthoquinone; right axis: (▽), 1,4-naphthoquinone; (◇), 1-naphthol; (○), 2-naphthol.

besides predominant oligomeric compounds. Formation of polymeric products resulting from naphthols was reported by Boyland and Sims [9] for a Fenton reaction system ($FeSO_4/H_2SO_4/H_2O_2$).

3.2. Photocatalytic degradation of naphthalene in Q-TiO_2 colloidal solutions

3.2.1. Course of the degradation

Colloidal solutions of Q-TiO_2 particles were characterized by UV–VIS spectroscopy. In Fig. 4, absorption spectra of 1×10^{-3} mol l^{-1} Q-TiO_2, freshly prepared as well as aged, are shown. The aging caused a red shift of approximately 5 nm indicating an increase of particle sizes with time.

Fig. 5 shows typical kinetic curves of the photocatalytic degradation of naphthalene (8.6×10^{-5} and 1.9×10^{-4} mol l^{-1}) in colloidal solution of Q-TiO_2 (4.8×10^{-4} mol l^{-1}). In contrast to the analogous process photoinduced by Fe(III), the kinetics of photocatalytic degradation of naphthalene in colloidal solution of Q-TiO_2 particles was found to be more complex, showing three different kinetic steps (first fast, second slow and

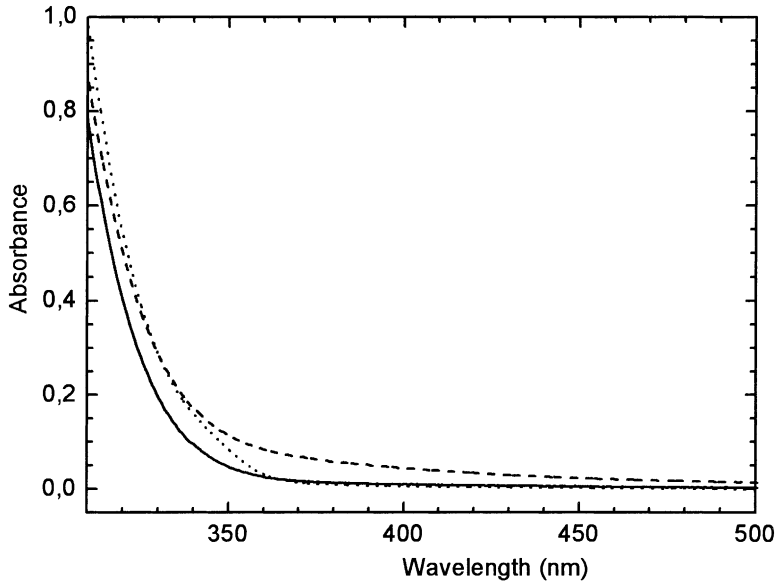

Fig. 4. Absorption spectra of 1.0×10^{-3} mol l^{-1} Q-TiO_2 in aqueous solution (pH = 2.5). Full line: freshly prepared particles; dotted line: aged particles, dashed line: spectrum of a solution containing freshly prepared Q-TiO_2 and 1.0×10^{-4} mol l^{-1} naphthalene after 225 min of irradiation.

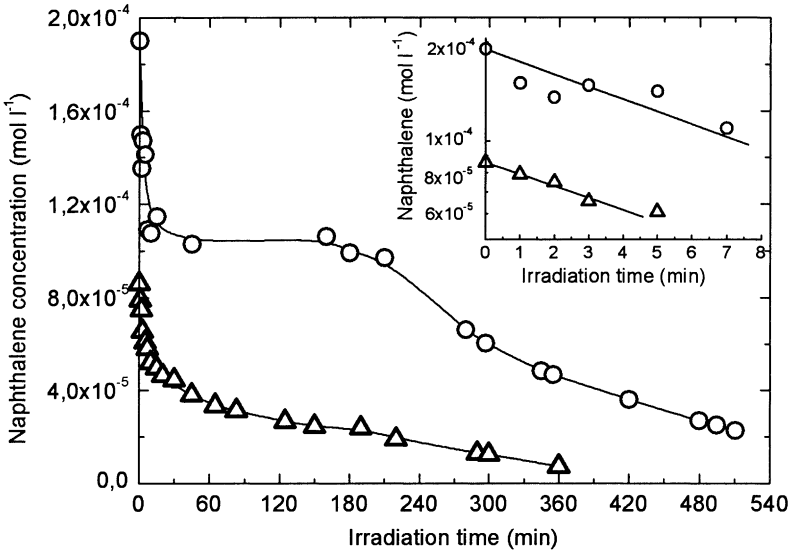

Fig. 5. Photocatalytic degradation of naphthalene in aged colloidal solutions of 4.8×10^{-4} mol l^{-1} Q-TiO_2. The irradiation intensity was $I_0 = 1.0 \times 10^{16}$ photons s^{-1} cm^{-3}. Initial concentrations of naphthalene: (△), 8.6×10^{-5} mol l^{-1}; (○), 1.9×10^{-4} mol l^{-1}. The insert represents first order fits of several initial experimental points.

third again faster). This behavior should not be related exclusively to the properties of Q-TiO_2 colloid, but also of naphthalene or of its degradation intermediates. When dealing with 4-chlorophenol [24] or diuron (3-(3,4-dichlorophenyl)-1,1-dimethyl urea) [25] under the same conditions, the degradation followed the first order kinetics well.

The initial fast stage of the naphthalene photocatalytic degradation could be approximated by the first order kinetics relations (see Fig. 5). After a short irradiation time, the reaction rate suddenly decreased causing almost constant middle stage of the kinetic curve. The degradation was inhibited more strongly for the higher concentration of naphthalene. Nevertheless, for the lower concentration of naphthalene, the slow second step can be still distinguished. During the third stage, the reaction rate increased again.

The complex kinetic behavior was accompanied with parallel spectral changes of the colloidal solution that, originally colorless, became yellow. A typical observed absorption spectrum is shown as a dashed curve in Fig. 4. Exact spectroscopic measurements showed that the absorbance at wavelengths below 600 nm was increasing during the first fast kinetic stage. Then it reached a maximum just at the irradiation time corresponding to the slow middle kinetic period. Later, the absorbance began to decrease correspondingly with the third faster kinetic step.

This observation could be explained by the formation of a charge-transfer complex of some of the degradation intermediates on the surface of Q-TiO_2 nanoparticles. An intermediate that is strongly adsorbed on semiconductor particles should be favored in competition with non-adsorbed organic components dissolved in aqueous phase of the photocatalytic reaction system. Nevertheless, its faster oxidation by hole transfer should not reduce the reaction rate of the naphthalene decomposition dramatically because of the generally low concentrations of degradation intermediates relatively to that of the starting compound. However, the marked plateau observed on the kinetic curves would indicate a more efficient influence than only kinetic competition in oxidative degradation. The charge-transfer surface complexation might cause such an effect [26]. Oxygen-containing groups like ≻CHOH, ≻C=O, and –COOH can coordinate titanium atoms on the surface of Q-TiO_2 particles. Molecules with such groups located in appropriate positions form surface charge-transfer complexes that exhibit red shifts in absorption spectra [17,27]. The ligands of these complexes could be reversibly oxidized by holes and reduced by electrons photogenerated in the semiconductor particles and thus cause a “short-circuit” effect. As a consequence, the photoactivity of such Q-TiO_2 particles with surface complexes will be drastically diminished and the overall reaction rate of the photocatalytic degradation will strongly decrease.

Surface complexation by an intermediate of the naphthalene degradation and its influence on the photocatalytic activity of Q-TiO_2 particles would explain the observed kinetic behavior. Results of the parallel spectroscopic measurements support this explanation.

Beside the concentration of naphthalene, also the concentration of Q-TiO_2 influenced the reaction rate of degradation. In the cases of low Q-TiO_2 concentration (below 1×10^{-3} mol l^{-1}), the degradation was even completely stopped for a certain irradiation period of time. If the concentration of photocatalyst increased, the reaction rate of degradation was slowed down in much less extent.

At lower irradiation intensity, 1.7×10^{15} photons s^{-1} cm^{-3}, the overall degradation proceeded much slower

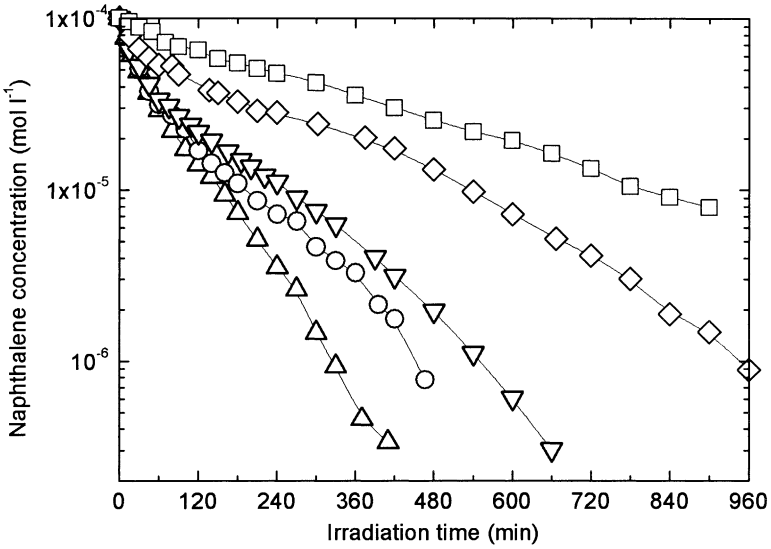

Fig. 6. Photocatalytic degradation of naphthalene (1.0×10^{-4} mol l^{-1}) in aged colloidal solutions of Q-TiO_2. Concentrations of Q-TiO_2: (△), 1.7×10^{-2} mol l^{-1}; (○), 1.0×10^{-2} mol l^{-1}; (▽), 7.0×10^{-3} mol l^{-1}; (◇), 5.0×10^{-3} mol l^{-1}; (□), 1.7×10^{-3} mol l^{-1}. The irradiation intensity was 1.7×10^{15} photons s^{-1} cm^{-3}.

and the kinetics became closer to the first order as can be seen in Fig. 6. However, the used semilogarithmic plot lets better distinguish three kinetic steps of particular degradation curves. The second slow stage shows a higher negative slope than the initial and the third period. The values of absorbance at 365 nm measured parallel in the course of the same set of experiments are shown in Fig. 7. The increase of the absorbance became faster and reached its maximum sooner for higher photocatalyst concentrations.

In the case of higher Q-TiO_2 concentrations, the absorbance began to decrease in the time corresponding to the start of the third stage of the naphthalene degradation curve. This may indicate that a surface complex that inhibited the activity of the photocatalyst, began to disappear due to the own degradation of the organic ligand. The lowering concentration of the surface complexes corresponds to the observed re-increase of the degradation rate of naphthalene.

The influence of the age of Q-TiO_2 on the photocatalytic degradation of naphthalene was also investigated. Experiments with 1.7×10^{-4} mol l^{-1} naphthalene in colloidal solution of 1.0×10^{-3} mol l^{-1} Q-TiO_2, both freshly prepared and aged, were carried out. The corresponding kinetic curves

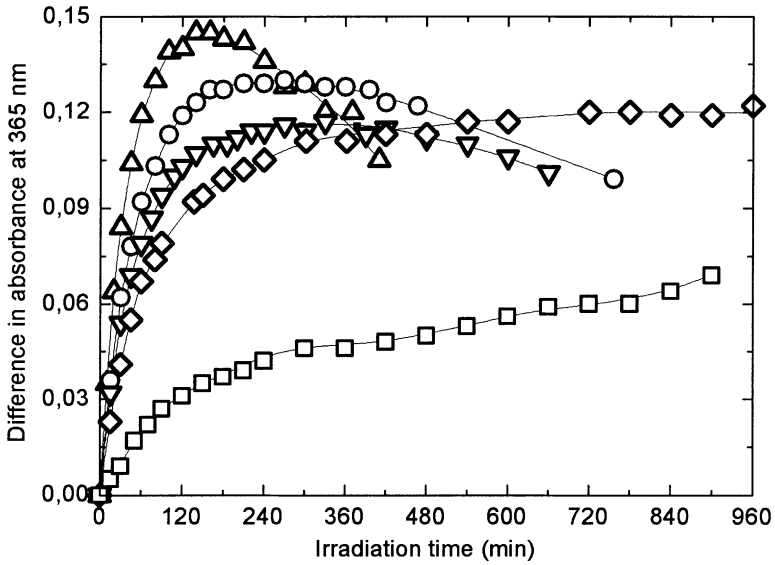

Fig. 7. Dependence of absorbance at 365 nm on irradiation time during photocatalytic degradation of naphthalene (1.0×10^{-4} mol l^{-1}) in aged colloidal solutions of Q-TiO_2. Concentration of Q-TiO_2: (△), 1.7×10^{-3} mol l^{-1}; (○), 1.0×10^{-2} mol l^{-1}; (▽) 7.0×10^{-3} mol l^{-1}; (◇), 5.0×10^{-3} mol l^{-1}; (□), 1.7×10^{-2} mol l^{-1}. The irradiation intensity was 1.7×10^{15} photons s^{-1} cm^{-3}.

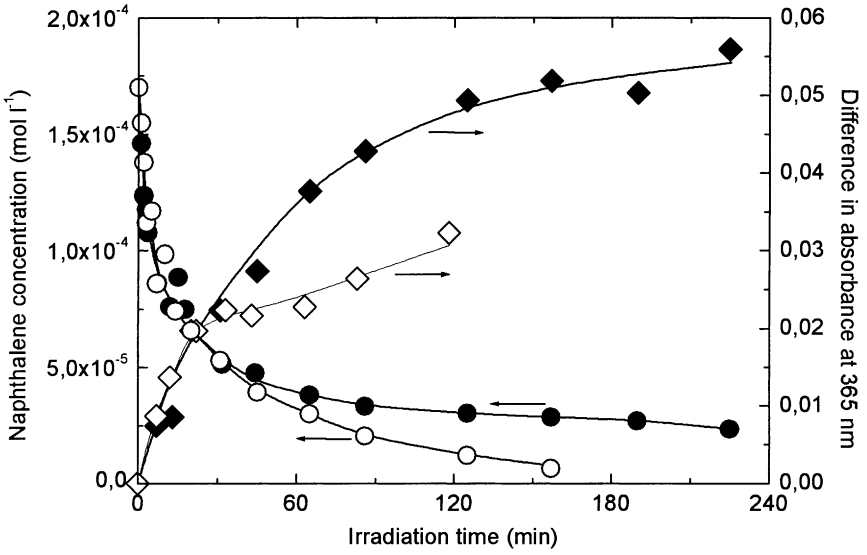

Fig. 8. Photocatalytic degradation of naphthalene (1.7×10^{-4} mol l^{-1}) in colloidal solutions of Q-TiO_2 (1.0×10^{-3} mol l^{-1}) and corresponding changes of absorbance at 365 nm: naphthalene degradation (●) and changes of absorption (◆) in freshly prepared Q-TiO_2 solution; naphthalene degradation (○) and changes of absorption (◇) in aged Q-TiO_2 solution. The irradiation intensity was $I_0 = 1.0 \times 10^{16}$ photons s^{-1} cm^{-3}.

are compared in Fig. 8. There were differences between the both cases: while the initial degradation rates obtained for the freshly prepared and aged Q-TiO_2 colloidal solutions were similar, the reaction rate corresponding to freshly prepared colloids was more decelerated during the middle stage. These kinetic effects were most probably caused by specific adsorption and formation of the surface complex with some of the degradation intermediates. In the case of the freshly prepared Q-TiO_2 particles, the absorbance grew higher than for the aged particles. A larger overall surface area of the freshly prepared colloid, which enabled to form higher concentration of the surface complex, caused probably this effect.

3.2.2. Influence of surface complexation on the course of photocatalytic degradation

It was reported that some substances, such as salicylic acid, form yellow charge-transfer complexes on the surface of colloidal Q-TiO_2 particles [28] and affect the photoelectrochemical behavior of TiO_2 layer electrodes. To verify the proposed relation between the surface complexation and the inhibited photocatalysis, spectral and photochemical tests were performed with *o*-coumaric acid. *o*-Coumaric acid has a structure similar to intermediates identified during photoinduced degradation of naphthalene: its lactone, coumarine, was found by Theurich et al. among intermediates of the photocatalytic degradation of naphthalene in TiO_2 slurries [6]. By the means of UV–VIS absorption spectroscopy, we observed a formation of surface complexes in colloidal solutions of Q-TiO_2 particles with coumaric acids.

A set of experiments was then carried out in which colloidal solutions of 1.0×10^{-2} mol l^{-1} Q-TiO_2 containing 1.0×10^{-4} mol l^{-1} naphthalene and various concentration of *o*-coumaric acid were irradiated ($I_0 = 1.7 \times 10^{15}$ photons s^{-1} cm^{-3}). It was found that the degradation of naphthalene became slower with increasing concentration of *o*-coumaric acid. The initial reaction rates were estimated by fitting several first experimental points of the corresponding kinetic curves using formally the first order kinetics. The obtained rate constants, k_{exp}, are summarized in Table 3. They are compared with expected theoretical values, k_{calc}. The latter parameters were calculated based on the assumptions that the initial reactions of hydroxyl radical with both naphthalene and *o*-coumaric acid were the rate determining steps of their own overall degradations and that these compounds only kinetically compete for OH-radical. Knowing the bimolecular rate constants of reactions of hydroxyl radical with both naphthalene and 2-coumarate anion, the pseudounimolecular rate constants k_{calc} could be calculated employing the procedure described in detail by Belháčová [29].

The experimental rate constants k_{exp} decreased with increasing concentration of *o*-coumaric acid but the decrease

Table 3
Experimental, k_{exp}, and calculated, k_{calc}, rate constants of photocatalytic degradation of naphthalene (1.0×10^{-4} mol l^{-1}) in colloidal solution of Q-TiO_2 (1.0×10^{-2} mol l^{-1}) containing various concentrations of *o*-coumaric acid

o-Coumaric acid (mol l^{-1})	k_{exp} (s^{-1})	k_{calc} (s^{-1})
0	$(3.7 \pm 0.3) \times 10^{-4}$	3.7×10^{-4}
1.0×10^{-7}	$(3.8 \pm 0.3) \times 10^{-4}$	3.7×10^{-4}
1.0×10^{-6}	$(3.1 \pm 0.2) \times 10^{-4}$	3.7×10^{-4}
3.0×10^{-6}	$(2.1 \pm 0.3) \times 10^{-4}$	3.6×10^{-4}
1.0×10^{-5}	$(9.8 \pm 1.5) \times 10^{-5}$	3.5×10^{-4}
3.0×10^{-5}	$(7.0 \pm 1.7) \times 10^{-5}$	3.1×10^{-4}

was greater than the corresponding calculated values k_{calc}. This fact could be attributed to the formation of charge-transfer complexes of *o*-coumaric acid on the surface of Q-TiO_2 particles. These complexes might cause the above mentioned "short-circuit" effect. Reversible charge transfers between semiconductor particle and coordinated ligands would formally increase quantum yield of the electron–hole recombination and thus cause the observed marked decrease of the initial reaction rate of photocatalytic degradation of naphthalene.

3.2.3. Intermediates of naphthalene degradation photocatalyzed by Q-TiO_2

The intermediates observed in the course of the photoinduced degradation of naphthalene in aqueous solutions of Fe(III) perchlorate (1-naphthol, 2-naphthol, 1,2-naphthoquinone, 1,4-naphthoquinone, 7-hydroxy-1,4-naphthoquinone, 2-formylcinnamaldehyde, phthalic acid) were also found during the photocatalytic degradation in colloidal solutions of Q-TiO_2 particles. Beside 2-formylcinnamaldehyde, hydroxylated derivative of 1,4-naphthoquinone was present in higher amounts, it indicates that 1,4-naphthoquinone was formed with higher reaction rate than in the case of the homogeneous photoinduced process. On the contrary, 1,2-naphthoquinone, which was found as a main intermediate during the photoinduced degradation in Fe(III) solutions both with natural pH and slightly acidified (1.0×10^{-2} mol l^{-1} $HClO_4$), appeared here only in small amounts.

Photocatalytic degradation of both isomers of naphthols led to the formation of polymeric intermediates but different from those observed during analogous photoinduced processes. Nevertheless, it can be concluded for the both cases that naphthols are not the only primary intermediates of the oxidative degradation of naphthalene induced by hydroxyl radical attack as proposed elsewhere [6].

3.3. Proposed mechanism of oxidative degradation of naphthalene

Based on the found primary intermediates, reaction pathways of the naphthalene degradation can be proposed. As a primary chemical step, the reaction of naphthalene with hydroxyl radical photogenerated both in the aqueous solution of Fe(III) and on the TiO_2 surface, can be put forward.

There are three symmetrically different positions of carbon atoms in the naphthalene molecule, C_1, C_2, and atoms common for both rings of naphthalene (C_9 and C_{10}). The probability of an electrophilic addition of hydroxyl radical should be proportional to the electron density on particular carbon atoms. It decreases in the order $C_1 > C_2 > C_{9,10}$. The addition of hydroxyl radical can theoretically lead to three isomeric OH-adducts, which are radicals of cyclohexadienyl type. Various mesomeric forms can be assumed, as structures (**VI**), (**VII**), and (**VIII**) proposed in Scheme 1. In aerated aqueous solutions, a reversible addition [30] of molecular oxygen usually follows. It can be directed to various carbon atoms according to the location of the odd electron. The formed peroxyl radicals, i.e. (**IX**), (**X**), **(XI)**, (**XII**), and **(XIII)**, then undergo further reactions according to the orientation of the peroxyl function with the odd electron localized on the terminal oxygen atom. If there is a short distance to hydrogen bounded to the carbon bearing hydroxyl group, as in the case of *anti*-oriented isomers (**X**) and (**XIII**), an elimination of hydroperoxyl radical probably proceeds. It leads to the rearomatization and formation of 1-naphthol or 2-naphthol, respectively, as shown in Scheme 1.

According to Theurich et al. [6], naphthols are the only primary products of the photocatalytic degradation of naphthalene. They should consecutively transform via next attacks of hydroxyl radical into secondary naphthodiols and further intermediates, including ring-opened structures. However, neither photoinduced, nor photocatalytic degradation of naphthols yielded products identical to those of naphthalene, as it was shown in our experiments. Moreover, the sum of the initial reaction rates of the formation of both naphthols calculated based on experimental data shown in Fig. 3 was found to be far lower than the initial reaction rate of the naphthalene disappearance. It would mean that transformations into naphthols only represented very minor reaction pathways.

Besides naphthols, some other components of the degradation mixture of naphthalene showed time profiles without induction period, which are typical for primary intermediates (i.e. thermally stable products resulting from only one attack of hydroxyl radical onto the starting molecule of naphthalene). Following own experimental findings and their comparison with literature data [6,15], 2-formylcinnamaldehyde, 1,2-naphthoquinone, and 1,4-naphthoquinone were estimated as the primary intermediates of the naphthalene degradation induced by hydroxyl radical attack. Possible reaction pathways of their formation are proposed in Schemes 2–4.

The mechanism in Schemes 2 and 3 proposes the formation of both 1,2-naphthoquinone and 1,4-naphthoquinone as a consequence of only one OH-attack. Peroxyl radicals (**IX**), (**X**), and (**XI**) undergo an intramolecular rearrangement to endoperoxyl radicals, e.g. (**XIV**), (**XV**), and (**XIX**). A further molecule of oxygen can add onto these endoperoxyl radicals into positions with odd electron producing corresponding endoperoxyl radicals, e.g. (**XVI**), (**XX**). An important aspect of the proposed mechanism is the occurrence of endoperoxides postulated previously by Pan et al. [30] to explain products found in pulse radiolysis of benzene in aqueous solution.

Some of the organic peroxyl radicals can eliminate hydroperoxyl radical ($HO_2^{\bullet}$) and thus form close-shell structures with even number of electrons, e.g. (**XVII**) and (**XXI**). Undergoing further intramolecular rearrangement, endoperoxides (**XVII**) and (**XXI**) are transformed to corresponding thermally stable primary intermediates. The endoperoxides typically split either only their O–O bond, forming,

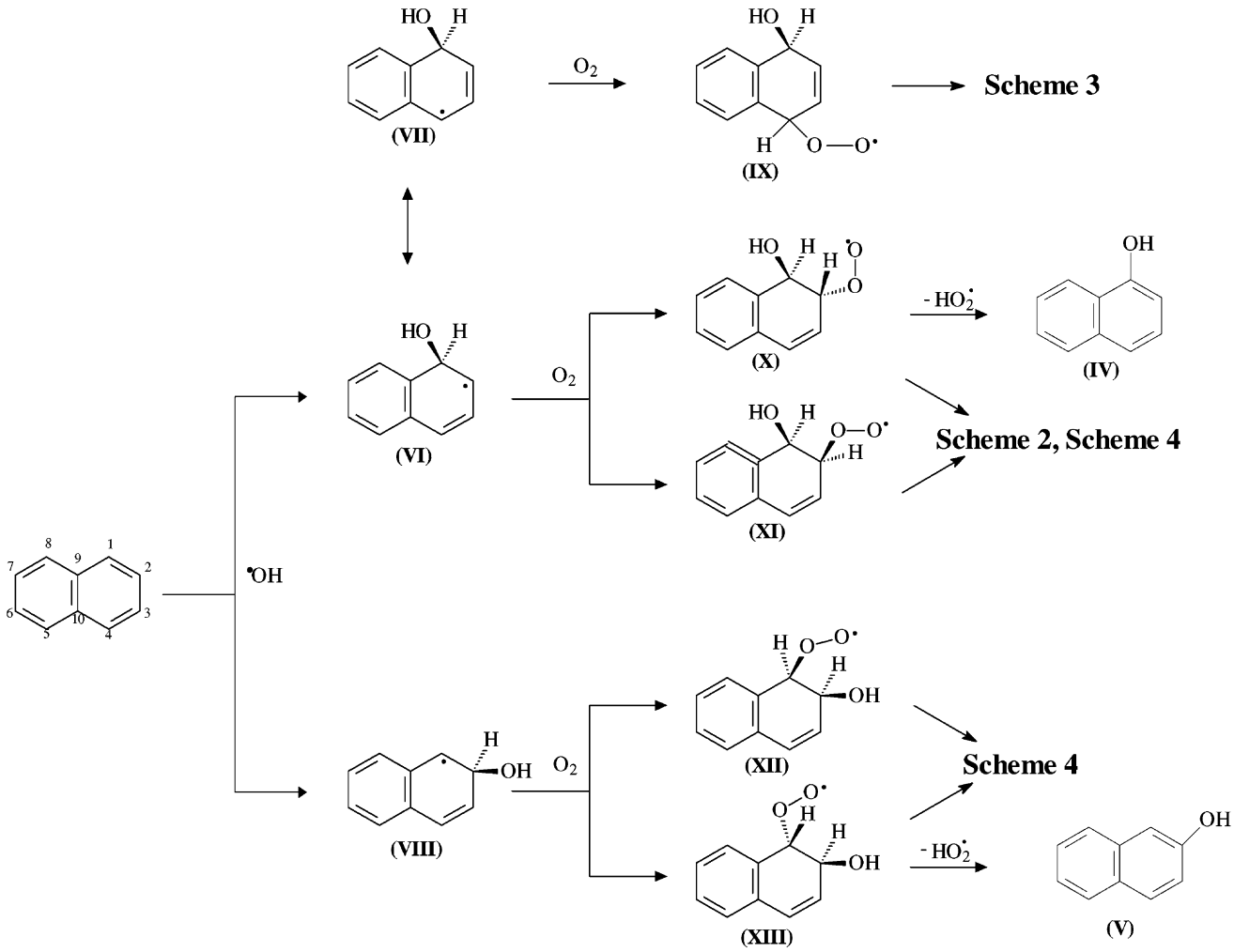

Scheme 1.

e.g. 1,2-naphthoquinone (**II**) and 1,4-naphthoquinone (**III**), or both O–O and C–C bonds, producing corresponding open-ring products [30].

Under conditions of both photoinduced and photocatalytic degradation, hydroperoxyl radical is probably the most common radical in the reaction system. It is produced not only by elimination from various peroxyl radicals described above but also in other reactions, e.g. electron transfer from TiO_2 particle to molecular oxygen and consecutive protonation. Because of the generally low reactivity of hydroperoxyl radical with organic substrates, its photostationary concentration should be the highest of all present radicals. That is why the termination reactions of organic radicals with hydroperoxyl radical are most probable. In this way, the formation of 2-formylcinnamaldehyde (**I**), the main intermediate of the naphthalene degradation, is proposed in Scheme 4. Unstable tetraoxides (**XXIII**) and (**XXIV**) that initially result from the termination reaction undergo further intramolecular rearrangements. Splitting of two O–O bonds and one C–C bond can directly lead to a stable open-ring structure. To support this proposed mechanism, theoretical calculations of the reaction coordinate were performed. Applying the semiempirical method AM1, the existence of the corresponding transition state was confirmed.

As a conclusion, formation of thermally stable intermediates, other than only naphthols, can result from the primary attack of hydroxyl radical onto naphthalene molecule. The formal oxidation stage of the particular product depends on the number of consecutive additions of oxygen and on the way of termination of the radical. Formally, addition of one hydroxyl radical increases the oxidation stage of the organic molecule equivalently to removing one electron. Each consecutive addition of oxygen formally removes four electrons. The elimination of hydroperoxyl radical lowers the oxidation stage equivalently to an addition of three electrons. In the termination reactions with hydroperoxyl radical, the oxidation stage is reduced equivalently to an addition of one electron. That is why, according to the specific reaction pathway, variously oxidized compounds can result from the initial OH-attack onto the naphthalene molecule, i.e. naphthols (formally two electrons removed), 2-formylcinnamaldehyde (four electrons), and naphthoquinones (six electrons).

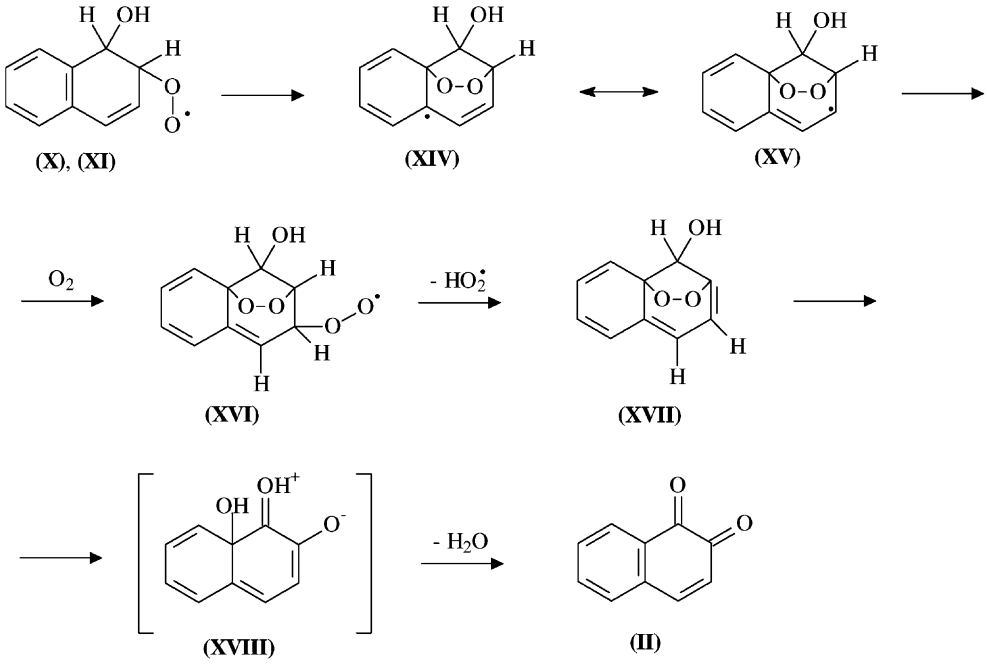

Scheme 2.

In homogeneous Fe(III) solutions, additional thermal oxidation reactions can occur. A mechanism explaining the found higher abundance of 1,2-naphthoquinone in the presence of Fe(III), compared to Q-TiO_2 solutions, is proposed in Scheme 5. It involves oxidation of carbon centered radicals, (**VI**) and (**VIII**), by Fe(III) in several consecutive steps.

All thermally stable primary intermediates undergo further reactions initiated by the second OH-attack. Besides addition of hydroxyl radical onto unsaturated bonds, also H-abstraction can proceed. Particularly, aliphatic hydrogen atoms of the open-ring structures, which resulted from the first OH-attack, are abstracted. Such organic radicals

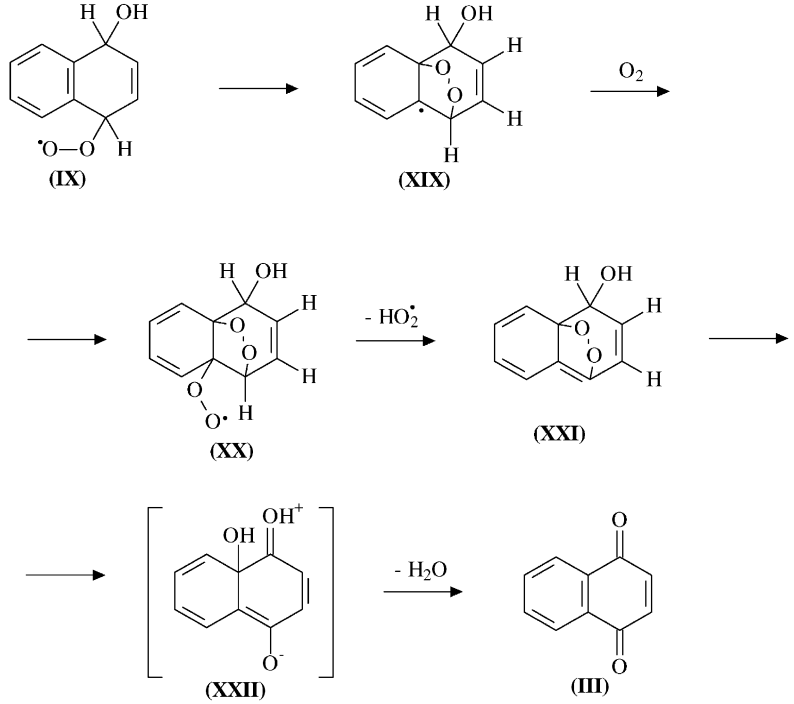

Scheme 3.

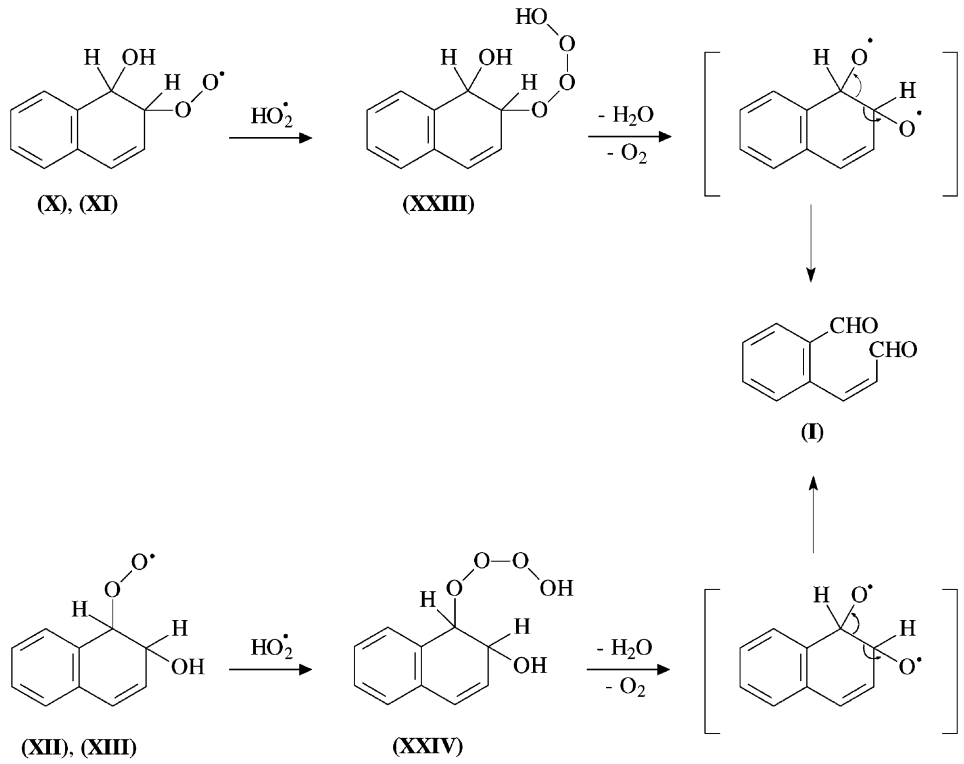

Scheme 4.

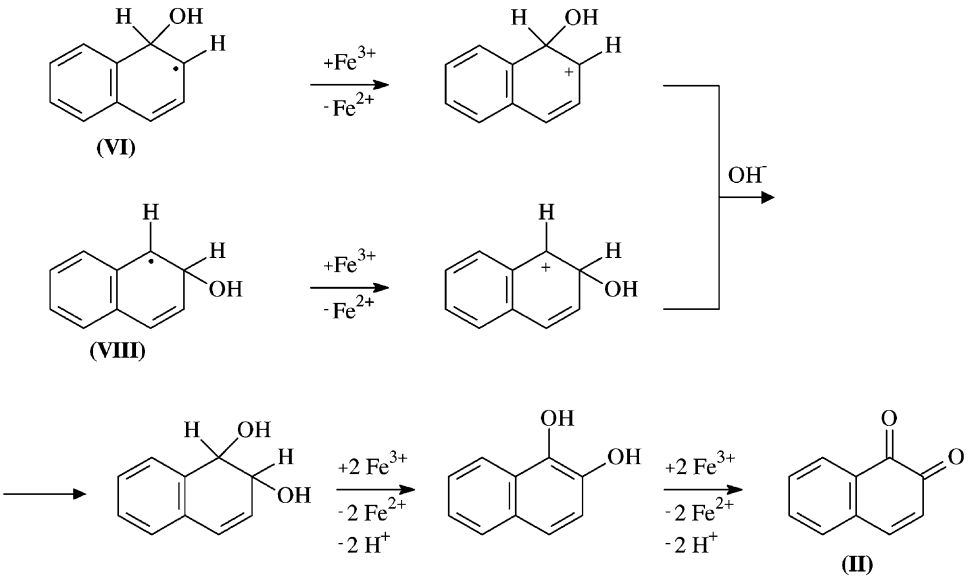

Scheme 5.

with odd electron localized on aliphatic carbon atoms appear. They typically add oxygen molecules forming aliphatic peroxyl radicals or reduce Fe(III). If the radical chain is terminated in reactions with hydroperoxyl radical, oxygen-containing derivatives are formed. As a conclusion, repeated OH-attacks (additions as well as H-abstractions) finally lead to total mineralization of naphthalene, i.e. to its complete transformation into carbon dioxide and water.

4. Conclusion

Oxidative degradation processes of naphthalene, both photoinduced in Fe(III) solutions and photocatalysed by Q-TiO_2 colloids, were investigated and compared. In homogeneous solutions of Fe(III) perchlorate, the degradation followed approximately the first order kinetics. Nevertheless, the rate constant was largely influenced by irreversible

hydrolytic processes occurring with Fe(III). The initial degradation rate of naphthalene was approximately proportional to concentration of the most photoactive monomeric Fe(III) species, i.e. $[Fe(H_2O)_5OH]^{2+}$, which generally decreased with the age of Fe(III) perchlorate solution. As for the heterogeneous photocatalytic system of colloidal solutions of Q-TiO_2 particles, a complex degradation kinetics with three different steps (first fast, second slow and third again faster) was observed. The deceleration during the middle stage was attributed to the formation of surface complexes with some of the naphthalene degradation intermediates. That is why the parameters such as light intensity, particle size and concentration of Q-TiO_2 photocatalyst and initial concentration of naphthalene influenced the degradation rate in a more complex way. The primary degradation intermediates (1-naphthol, 2-naphthol, 1,2-naphthoquinone, 1,4-naphthoquinone, 2-formylcinnamaldehyde) were the same for both systems. The reaction mechanism of the degradation was proposed, assuming the initial attack of hydroxyl radical followed by addition of dioxygen and elimination of hydroperoxyl radical. In the case of 1,2-naphthoquinone, an additional oxidation of its precursor by Fe(III) was considered to explain its higher abundance observed during the Fe(III) photoinduced process.

Acknowledgements

This work was supported by the French-Czech Cooperation Program Barrande, project 98086, by the NATO Science Program, Collaborative Linkage Grant 975828, and by the Grant Agency of the Czech Republic, grants 203/99/0763 and 203/01/D145. L. Hykrdová also thanks the French Government for allocation of a scholarship to her internship in France.

References

[1] B.C. Faust, J. Hoigné, J. Atmos. Environ. 24A (1990) 79.
[2] R.J. Knight, R.N. Sylva, J. Inorg. Nucl. Chem. 37 (1975) 779.
[3] M. Sarakha, personal communication.
[4] M. Grätzel, Heterogeneous Photochemical Electron Transfer, CRC Press, Boca Raton, FL, 1989.
[5] E. Pramauro, A. Bianco Prevot, M. Vincenti, R. Gamberini, Chemosphere 36 (1998) 1523.
[6] J. Theurich, D.W. Bahnemann, R. Vogel, F.E. Ehamed, G. Alhakimi, I. Rajab, Res. Chem. Intermed. 23 (1997) 247.
[7] S. Das, M. Muneer, K.R. Gopiodas, J. Photochem. Photobiol. A 77 (1994) 83.
[8] F. Soana, M. Sturini, L. Cermenati, A. Albini, J. Chem. Soc., Perkin Trans. 2 (2000) 699.
[9] F. Boyland, P. Sims, J. Phys. Chem. 48 (1953) 2967.
[10] T.A. Tukhanen, F.J. Beltrán, Chemosphere 30 (1995) 1463.
[11] N.J. Bunce, L. Liu, J. Zhu, D.A. Lane, Environ. Sci. Technol. 31 (1997) 2252.
[12] D.A. Lane, H. Tang, Polycyclic Arom. Comp. 5 (1994) 131.
[13] D.A. Lane, S.S. Fielder, S.J. Townsend, N.J. Bunce, J. Zhu, L. Liu, P. Wiens, P. Pond, Polycyclic Arom. Comp. 9 (1996) 53.
[14] J. Sasaki, S.M. Aschmann, E.S.C. Kwok, R. Atkinson, J. Arey, Environ. Sci. Technol. 31 (1997) 3173.
[15] D. Vialaton, C. Richard, D. Bagho, A. Paya-Perez, J. Photochem. Photobiol. A 123 (1999) 15.
[16] C. Kormann, D.W. Bahnemann, M.R. Hoffmann, J. Phys. Chem. 92 (1998) 5196.
[17] M. Heyrovský, J. Jirkovský, M. Štruplová-Bartáčková, Langmuir 11 (1995) 4300.
[18] J.G. Calvert, J.M. Pitts, in: Photochemistry, Wiley, New York, 1966, p. 783.
[19] J. Butler, F.F. Jayson, A.J. Swallow, J. Chem. Soc., Faraday Trans. I 70 (1974) 1394.
[20] B.H.J. Bielski, D.E. Cabelli, R.L. Arudi, A.B. Ross, J. Phys. Chem. Ref. Data 14 (1985) 1041.
[21] P. Mazellier, J. Jirkovský, M. Bolte, Pestic. Sci. 49 (1997) 259.
[22] G.V. Buxton, C.L. Greenstock, W.P. Helman, A.B. Ross, J Phys. Chem. Ref. Data 17 (1988) 513.
[23] P. Mazelier, G. Mailhot, M. Bolte, New J. Chem. 21 (1997) 398.
[24] J. Jirkovský, personal communication.
[25] K. Macounová, H. Krýsová, J. Ludvík, J. Jirkovský, J. Photochem. Photobiol. A: Chem., submitted for publication.
[26] D.W. Bahnemann, M. Hilgendorff, R. Memming, J. Phys. Chem. B 101 (1997) 4265.
[27] J. Moser, S. Punchihewa, P.P. Infelta, M. Grätzel, Langmuir 7 (1991) 3012.
[28] K. Kratochvilová, I. Hoskovcová, J. Jirkovský, J. Klíma, J. Ludvík, J. Electrochim. Acta 40 (1995) 2603.
[29] L. Belháčová, Ph.D. Thesis, Prague, 2001.
[30] X.-M. Pan, M.N. Schuchman, C. Sonntag, J. Chem. Soc., Perkin Trans. 2 (1993) 289.